

Frequency-domain analysis of dynamically applied strain using sweep-free Brillouin time-domain analyzer and sloped-assisted FBG sensing

Asher Voskoboinik,^{1,*} Dvora Rogawski,¹ Hao Huang,¹ Yair Peled,² Alan E. Willner,¹ and Moshe Tur²

¹Department of Electrical Engineering-Systems, University of Southern California, 3740 McClintock Avenue, Los Angeles, CA, 90035, USA

²School of Electrical Engineering, Tel Aviv University, Ramat Aviv, 69978, Israel
voskoboi@usc.edu

Abstract: Fast reconstruction of the whole Brillouin gain spectrum is experimentally demonstrated using sweep-free Brillouin optical time-domain analysis (SF-BOTDA). Strain variations with the frequencies up to 400Hz are spectrally analyzed, achieving strain sensitivity of 1 microstrain per root Hz at a sampling rate of 5.5kHz and a spatial resolution of 4m. The results favorably compare with fiber Bragg grating sensing.

©2012 Optical Society of America

OCIS codes: (060.2330) Fiber optics communications; (060.2370) Fiber optics sensors.

References and links

1. X. Bao and L. Chen, "Recent progress in Brillouin scattering based fiber sensors," *Sensors (Basel)* **11**(4), 4152–4187 (2011).
2. S. Diaz, S. Mafang, M. Lopez-Amo, and L. Thevenaz, "A high performance optical time-domain Brillouin distributed fiber sensor," *IEEE Sens. J.* **8**(7), 1268–1272 (2008).
3. S. M. Foaleng, M. Tur, J. C. Beugnot, and L. Thevenaz, "High spatial and spectral resolution long-range sensing using Brillouin echoes," *J. Lightwave Technol.* **28**(20), 2993–3003 (2010).
4. W. Li, X. Bao, Y. Li, and L. Chen, "Differential pulse-width pair BOTDA for high spatial resolution sensing," *Opt. Express* **16**(26), 21616–21625 (2008).
5. T. Sperber, A. Eyal, M. Tur, and L. Thevenaz, "High spatial resolution distributed sensing in optical fibers by Brillouin gain-profile tracing," *Opt. Express* **18**(8), 8671–8679 (2010).
6. A. W. Brown, B. G. Colpitts, and K. Brown, "Dark-pulse Brillouin optical time-domain sensor with 20-mm spatial resolution," *J. Lightwave Technol.* **25**(1), 381–386 (2007).
7. Y. Antman, N. Primerov, J. Sancho, L. Thevenaz, and A. Zadok, "Localized and stationary dynamic gratings via stimulated Brillouin scattering with phase modulated pumps," *Opt. Express* **20**(7), 7807–7821 (2012).
8. R. Bernini, A. Minardo, and L. Zeni, "Dynamic strain measurement in optical fibers by stimulated Brillouin scattering," *Opt. Lett.* **34**(17), 2613–2615 (2009).
9. K. Y. Song, M. Kishi, Z. He, and K. Hotate, "High-repetition-rate distributed Brillouin sensor based on optical correlation-domain analysis with differential frequency modulation," *Opt. Lett.* **36**(11), 2062–2064 (2011).
10. J. Urricelqui, A. Zornoza, M. Sagues, and A. Loayssa, "Dynamic BOTDA measurements based on Brillouin phase-shift and RF demodulation," *Opt. Express* **20**(24), 26942–26949 (2012).
11. Y. Peled, A. Motil, L. Yaron, and M. Tur, "Slope-assisted fast distributed sensing in optical fibers with arbitrary Brillouin profile," *Opt. Express* **19**(21), 19845–19854 (2011).
12. Y. Peled, A. Motil, and M. Tur, "Fast Brillouin optical time-domain analysis for dynamic sensing," *Opt. Express* **20**(8), 8584–8591 (2012).
13. A. Voskoboinik, J. Wang, B. Shamee, S. Nuccio, L. Zhang, M. Chitgarha, A. Willner, and M. Tur, "SBS-based fiber optical sensing using frequency-domain simultaneous tone interrogation," *J. Lightwave Technol.* **29**(11), 1729–1735 (2011).
14. A. Voskoboinik, O. F. Yilmaz, A. W. Willner, and M. Tur, "Sweep-free distributed Brillouin time-domain analyzer (SF-BOTDA)," *Opt. Express* **19**(26), B842–B847 (2011).
15. A. Voskoboinik, A. Bozovich, A. E. Willner, and M. Tur, "Sweep-free Brillouin optical time-domain analyzer with extended dynamic range," CLEO-2012, San Jose, USA, May 2012.
16. A. Voskoboinik, H. Huang, Y. Peled, A. E. Willner, and M. Tur, "Frequency-domain analysis of dynamically applied strain using sweep-free Brillouin time-domain analyzer," ECOC-2012, Amsterdam, Netherlands, September 2012.
17. J. Proakis and D. Manolakis, *Digital Signal Processing*, (Pearson Prentice Hall, 2007).

1. Introduction

Brillouin optical time domain analysis (BOTDA) [1,2] is now successfully applied to a variety of security and structural health monitoring applications, requiring a distributed sensing of temperature/sensing with good distance resolution ($<1\text{m}$ in most commercial instruments) [3–7]. Its current most prevalent implementations involve sweeping the optical frequency of a pump pulse against a continuous wave (CW) probe wave, thereby determining the Brillouin gain spectrum, whose peak is a measure of the local temperature/strain. This sweeping/scanning process is rather slow but it does not limit long range (50km) scenarios, where quite long averaging is required. Short range sensing may suffer from this slow scanning, limiting the application semi-static situations. Quite a few approaches have been recently proposed to extend BOTDA to the dynamic domain, reaching 1kHz distributed sensing and beyond [8–12].

Recently [13,14], we proposed a technique which completely eliminates this frequency sweeping by replacing the two interacting waves with properly matched multiple probe and pump tones. Clearly, the simultaneous use of multiple tones should shorten the sensing time by the factor equals to the number of optical tones used for interrogation. After demonstrating distributed sensing [14] using our Sweep-Free BOTDA (SF-BOTDA) and exploring its dynamic range [15], we extend our preliminary results of [16] and demonstrate distributed monitoring of temporally dynamic events, including spectral analysis, with frequencies up to 400Hz and a spatial resolution of 4m along a single-mode optical fiber. The results are now also compared to those obtained using a fiber Bragg grating (FBG).

2. Description of method

The concept of the SF-BOTDA sensor [13,14] is shown in Fig. 1. Multiple pumps and multiple probe tones are propagated in opposite direction. Each pump induces its own Brillouin gain spectrum (BGS). The probe optical frequencies are chosen to probe different parts of the corresponding Brillouin gain spectra, and therefore they frequency spacing between probe-pump pairs follow an arithmetic series, whose difference defines the granularity at which the BGS may be eventually reconstructed. As depicted in Fig. 1, the i -th tone of the pump amplifies the i -th tone of the probe. In our example, the frequency spacing of the pump tones is chosen to be 100MHz, while the frequency spacing of the probe tones is 103 MHz. In this way, the frequency difference between pump and probe tones decreases by 3MHz from the i -th to the $(i + 1)$ -th. Clearly, different probe tones experience different Brillouin amplification, making it possible to simultaneously measure the shape of the whole BGS, and eliminating the need for time-consuming frequency sweeping. In order to achieve spatial resolution, the multiple pump tones are pulsed in sequential manner [14] in order to minimize unwanted nonlinear interactions among the high power pump tones.

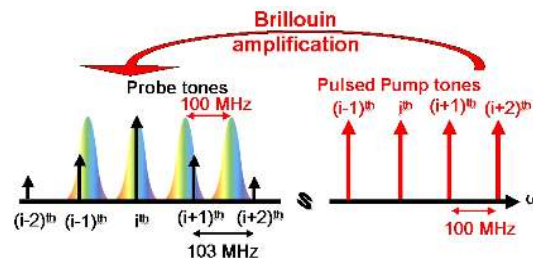


Fig. 1. BGS reconstruction using SF-BOTDA in a single multiple pump multiple probe measurement.

3. Experimental setup

A block diagram of SF-BOTDA experimental setup is shown in Fig. 2(a) and it is basically very similar to the one in [16]. A 80kHz linewidth laser is split into two arms, pump and

probe. A wideband arbitrary waveform generator (AWG) produces two different radio-frequency (RF) frequency combs, comprising N tones, one for the pump and the other for the probe tones. For the probe arm, this RF signal feeds an RF mixer at its intermediate frequency (IF) input, while its local oscillator (LO) input is driven by a microwave source, running at approximately the BFS of the fiber and is set to be 10914MHz. The mixer output comprises $2N$ RF tones, symmetrically located around 10914MHz. This signal is now further amplified (to compensate for poor up-conversion efficiency) and fed into MZM1 (Mach-Zehnder modulator), operating at its quadrature point, where the tones are translated to the optical domain, generating two optical multiple-tone sidebands ($2N$ -tone each) around the optical carrier frequency.

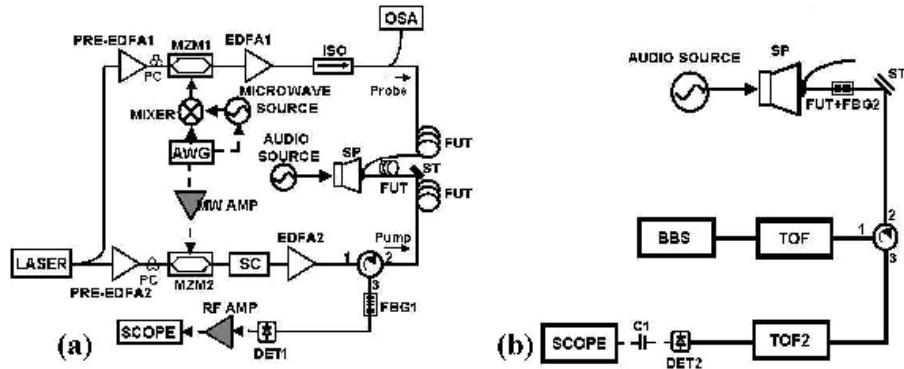


Fig. 2. Experimental setups: (a) MZM: Mach-Zehnder EO modulator; EDFA: Erbium-doped fiber amplifier; PC: Polarization controller; SC: Polarization scrambler; ISO: Optical isolator; DET1: detector; FBG1: Fiber Bragg grating filter; RF AMP: radio-frequency amplifier; MW AMP: Microwave frequency amplifier; AWG: Arbitrary waveform generator; SCOPE: Real-time acquisition system; OSA: Optical spectrum analyser; FUT: fiber-under-test; SP: Speaker, ST2: Translation stage. (b) BBS: Broadband source; TOF: Tunable optical filter; C1: capacitor.

The lower sideband serves as the optical probe, while the upper side band is eventually removed by the FBG1 – fiber Bragg grating filter. For the pump arm, another channel of the AWG generates the required complex signal, comprising a compact sequence of equally-wide sub-pulses, each riding on a different pump optical carrier [14]. Modulator MZM2, operating at its zero-transmission point to suppress the laser carrier, is fed with the RF pump pulse train. The sequential launching of the pump tones results in time-shifted Brillouin-amplified probe tones traces, which are later realigned at the processing stage by a simple temporal correction [14]. An Erbium-doped fiber amplifier (PRE-EDFA2), preceding MZM2, serves to reach the maximum allowed input power into MZM2. From MZM2 the pump signal continues to EDFA2 for further amplification, and finally to the fiber under test (FUT), comprising ~30m of SMF-28 fiber. The middle 6m section of this fiber was stretched between the center of the membrane of an audio speaker (SP) and a fixed stage. This fiber section could then be subjected to dynamic strain through electrical excitation of the speaker. A narrow linewidth fiber Bragg grating (4GHz) in the setup is used to precisely block the upper optical sideband, without attenuating the co-propagating laser frequency that serves as LO in a heterodyne detection. After the Brillouin amplification, the probe signal hits a wideband detector, where it mixes with the laser signal that co-propagated with it along the fiber. The resulting ~11GHz electrical signal is amplified by an RF amplifier and sent to a fast 20GHz bandwidth real-time acquisition system for digitization and further post-processing. In the experiment, ten ($N = 10$) RF tones were used for the pump signal where each sub-pulse length was 40ns to obtain 4m of spatial resolution. The chosen RF pump tone frequencies were 105, 240, 390, 525, 670, 810, 955, 1090, 1230 and 1370 MHz. This unequal spacing is used to reduce the detrimental effect of inter-modulation products. The chosen RF probe tone frequencies were 102, 234, 381, 513, 655, 792, 934, 1066, 1203 and 1340MHz, respectively, having a 3-MHz spacing decrement relative to the pump tone spacing. After up-conversion, the resulting optical probe

comb included 20 different frequencies located around 10914MHz and spanning a sweep-free range of 60MHz with a 3MHz resolution.

An independent measurement of the displacement of speaker's membrane, missing in [16], was achieved with the help of a parallel fiber attached between the speaker's membrane and a moving stage (ST2), Fig. 2(b). This 40cm fiber included a fiber Bragg grating (FBG2) whose 4GHz narrow transmission window moved in unison with the membrane. The frequency position of the vibrating spectral transmission window of FBG2 was recorded by shining FBG2 with a broadband source and detecting the returned optical signal from FBG2 after it passed through a tunable optical filter (TOF2), whose transmission in the region of interest varies with frequency as in Fig. 3. By working on the linear part of the slope of Fig. 3, a good estimate of the membrane displacement can be obtained, from which the strain of the FUT can be independently calculated. A broadband ASE source (BBS) was used. It first entered a tunable optical filter (TOF), whose central frequency was set to match the center frequency of the free FBG2 and its spectral width to match the expected strain variations to be later applied to FBG2. The output of the tunable filter was fed to FBG2. Before turning the speaker on the two fibers had to be somewhat pre-stretched in order to accommodate negative strains without getting the fibers loose. The tunable filter (TOF2) had a linear slope across $\sim 2.6\text{nm}$ and its -3dB point was set to fall on the central wavelength of the stretched FBG2 while the speaker was off. Having in mind that FBG2 wavelength-to-strain coefficient is around $1.2\text{pm}/\mu\epsilon$, the width of the linear slope of TOF2 determines the total dynamic range to be around $2100\mu\epsilon$. When the speaker is on, its membrane moves the center frequency of FBG2 back and forth and this spectral shift is translated by TOF2 and the following detector and the RC-based ($1\text{M}\Omega$, $5\mu\text{F}$) low pass filter to voltage variations. This measured membrane displacement may be interpreted as the “input” to the “system” of the Brillouin sensor, whose response is considered as the “output”.

To save memory on the data acquisition system, we employed down sampling techniques and sampled the $\sim 11\text{GHz}$ signal at 6.25GSamples/s . Such sub-Nyquist sampling creates an isolated replica of the probe baseband signal around 1.5GHz ($= |11-2*6.25|$). Since the bandwidth of the signal was only $\sim 2.7\text{GHz}$ [$2*\text{Highest tone used}$ ($= 1370\text{MHz}$)], a 3GHz RF filter can recover the signal with no aliasing [17]. Segmented memory was used to capture a $1\mu\text{sec}$ record for every $15\mu\text{sec}$. The total number of triggered records ($= 1668$), was divided into 834 pairs, whose first member documents the Brillouin amplified probe signal from the whole fiber (with the pump on), while the second member records the trace with the pump off. Then, every six records were averaged into a single one, resulting in an effective sampling rate of 555 records per second for a total recording period of 25ms. Then, each record was Fourier transformed in 40ns sections to obtain the heights of the various amplified probe tones, from which, after proper normalization with the no-pump trace, the BGS was reconstructed and the time evolution of the BFS was determined.

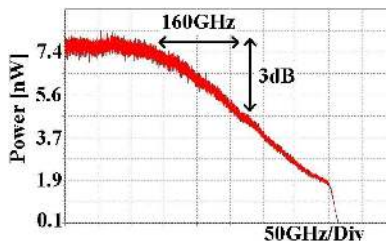


Fig. 3. Transmission characteristics of TOF2 showing a 3dB bandwidth of $\sim 160\text{GHz}$.

4. Results and discussion

The response of FBG2 (i.e., the spectral variations of reflection peak) while a 100Hz signal was applied to the speaker is shown in Figs. 4. The noise in Fig. 4(a), which originates from the ASE-based BBS, is largely attenuated by the RC filter, Fig. 4(b). The responses of the SF-

BOTDA and FBG2 sensors were simultaneously measured, while various signals were applied to the speaker. These signal tones were chosen to match (i.e., be multiples of) our SF-BOTDA 40Hz (1/25ms) spectral resolution, currently limited by the memory depth of the real-time scope. Figures 5(a)-5(c) and Figs. 6(a)-6(c) show the results of measuring a single 80Hz tone. Figures 5(a) and 6(a) show the time-domain and frequency-domain inputs to the speaker. Figures 5(b) and 6(b) show the response FBG2, whereas Figs. 5(c) and 6(c) show those of the rather wideband SF-BOTDA sensor, after 200Hz low-pass digital filtering. Figures 5(d)-5(f) and Figs. 6(d)-6(f) describe the response to a 120Hz single tone. Finally, Figs. 5(g)-5(i) and Figs. 6(g)-6(i) describe the case where a multitone signal, originating from the FM modulation of a 120Hz carrier with a 40Hz tone is applied to the speaker. The strain induced on the FBG2 is estimated from the SF-BOTDA measurement considering length ratio between SF-BOTDA and FBG2 FUTs.

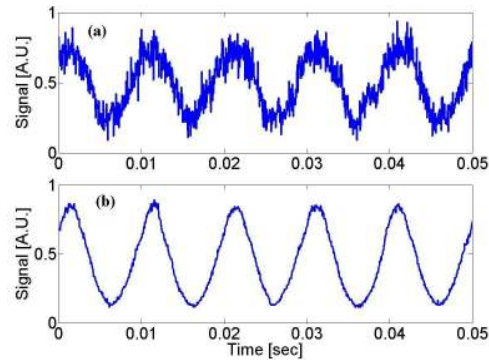


Fig. 4. The detector voltage when the speaker membrane is driven by a 100Hz signal before (a) and after (b) RC filtering.

We first note that the speaker's response to the input signal is slightly distorted, probably as a result of the mechanical load presented by the two stretched fibers. As for the actual measured membrane displacement-induced strains, in all cases the SF-BOTDA results are in good agreement with the FBG2 data. Differences do exist and we believe they are due to the fact that FBG2 is part of a *parallel* fiber, rather than of the FUT used for the SF-BOTDA measurements. In principle, an improved configuration, where FBG2 is an integral part of the SF-BOTDA FUT, is possible using different non-overlapping spectral windows for the Brillouin and Bragg interrogations and a dedicated FBG sensing equipment. With the known [6] conversion factor of 50kHz/ $\mu\epsilon$, the observed peak-to-peak amplitude of the induced BFS vibrations (~ 1.5 MHz), we were measuring strains of the order of $30\mu\epsilon$. Spectral analysis of the signals is presented in Fig. 5, indicating a BFS signal to noise ratio of ~ 20 dB (@80-200Hz) for a noise bandwidth of 40Hz (1/25ms), which is equivalent to a strain sensitivity of $\sim 1\mu\epsilon$ per root Hz.

It has been determined that the displacement of the speaker's membrane decreased with applied frequency. Consequently, high frequency strains were more difficult to measure with our setup. Figure 6(j) shows the recording of 400Hz single tone with calibrated microphone together with the response of the SF-BOTDA sensor, displaying poorer performance.

5. Conclusions

We have successfully demonstrated for the first time the ability of an SF-BOTDA setup to measure fast varying phenomena at an effective sampling rate of 5.5kHz. Results were favorably compared with parallel strain readings from an FBG. Strain variations of up to 400Hz were recorded and their spectral characteristics analyzed, achieving a strain sensitivity of $\sim 1\mu\epsilon/\sqrt{\text{Hz}}$. Improvement of the setup sensitivity and the determination of its limitations are under current research.

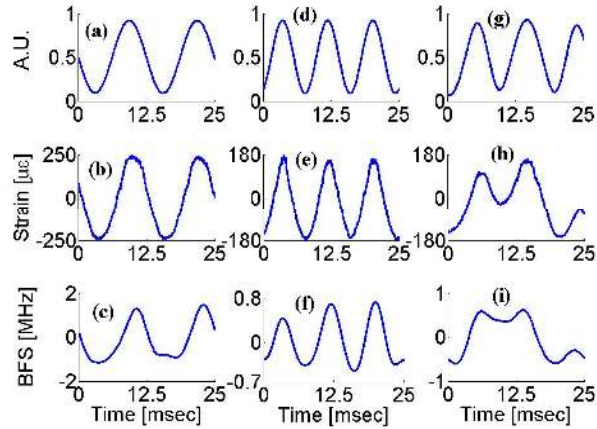


Fig. 5. The time-domain results of single tone input as measured at 80 and 120Hz (a,d) before speaker (b,e) using FBG, (c,f) using SF-BOTDA after 200Hz low-pass digital filtering. The time-domain results of FM modulated 120Hz signal with 40Hz span as measured (g) before speaker, (h) using FBG, (i) using SF-BOTDA and digitally processed.

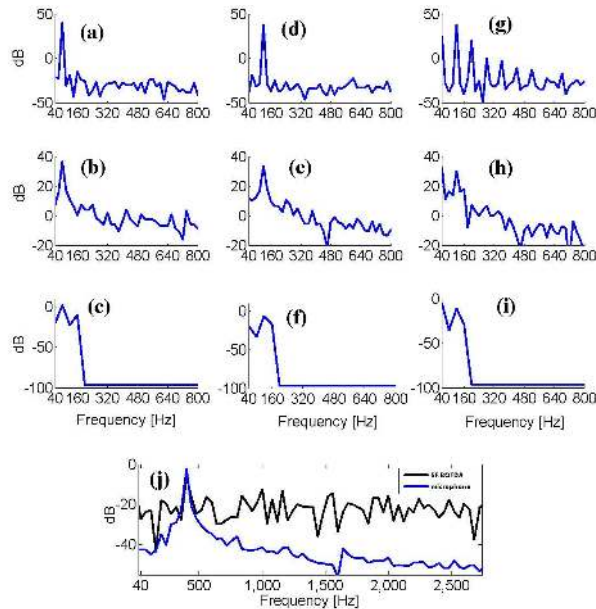


Fig. 6. The frequency-domain results for 80Hz, 120Hz and multitone excitations (a,d,g) before speaker (b,e,f) using FBG, (c,f,i) using SF-BOTDA after 200Hz low-pass digital filtering. (j) The results of measuring 400Hz single tone using SF-BOTDA and output of speaker with calibrated microphone.

Acknowledgments

We acknowledge the support of the Defense Security Cooperation Agency (DSCA) under contract DSCA-4440145260.